American Mineralogist, Volume 65, pages 733–745, 1980

Volume behavior of silicate solid solutions

ROBERT C. NEWTON AND BERNARD J. WOOD

Department of the Geophysical Sciences, University of Chicago
Chicago, Illinois 60637

Abstract

The characteristic form of the molar volume curve for binary silicate solid solutions is S-shaped, rather than linear or near-linear. The region of negative deviation from linearity is always close to the small-volume end-member, with positive departures near the large-volume end.

A *Non-Equivalent Site* (NS) type of volume behavior is a broad sigmoid that arises from the presence of some crystallographic sites in a structure larger than others capable of accepting the same large substituting cation(s). Initial substitution of the large-volume component into the smaller-volume end-member has only a small effect on the unit-cell volume until the large "easy" sites are saturated, which occurs at a rational mole fraction. Then a region of positive excess volumes follows more or less abruptly. Examples are (Na,K) nephelines and (Mg,Fe^{2+}) amphiboles.

An *Equivalent Site* (ES) volume behavior occurs in systems where, because of nearly identical sites accepting a certain substituting cation, there are no preferred "easy" sites. The first small substitution of the larger-volume component produces only local deformations without expansion of the structure as a whole, giving rise to a sharply-curving region of negative excess volume, usually within ten mole percent of the small-volume end-member. Examples are the (Fe^{2+},Ca) and (Mg,Ca) garnets, and, probably, the alkali feldspars and olivines.

The volume sigmoid is less common among non-silicates. It is shown by some oxide systems, *e.g.* (Mg,Fe^{2+}) ilmenites (ES) and magnetite–ulvöspinel (NS).

Thermodynamic excess quantities such as excess entropy, enthalpy, and free energy may be closely related to the volume curves. Possible examples are excess entropy in high alkali feldspars and excess free energy in (Fe^{2+},Ca) garnets.

Introduction

Volume relationships in binary solid solutions are often regarded as good indicators of the general thermodynamic properties of the solution series. If, for example, there is a linear (ideal) relationship between volume and composition, this is sometimes regarded as evidence of ideal behavior in a thermochemical sense also (*e.g.* Hess, 1952, p. 183).

Kerrick and Darken (1975) noted that the larger the difference in volumes between end-members of a binary series, the greater the tendency away from ideal solution behavior, with excess (non-proportional) enthalpy, free energy, and, possibly, entropy of mixing, as well as excess volume of mixing. In many cases all of the mixing functions, including volume of mixing, have been fitted with second or third degree polynomial equations (Thompson, 1967) which satisfy the conditions of approach to Henry's Law behavior at infinite dilution of a component and approach to Raoult's Law (proportional) behavior as the concentration of the component approaches unity.

This type of fitting has the advantage of rendering the non-ideal excess volume in a convenient form for thermodynamic computation but has the disadvantage that little insight into the specific structural controls of solid-solution behavior is offered. Another problem is that small-scale but significant deviations from the assumed simple relationship are often obscured. Small-scale molar volume "events" may be important for calculation of high-pressure phase equilibria because of steepened tangents to the volume–composition curve, with corresponding increase or decrease of the activities of the solution components at high pressures. Thus, Cressey *et al.* (1978) chose to draw molar volume and partial

0003–004X/80/0708–0733$02.00

molal volume curves by eye for the garnet join $Fe_3Al_2Si_3O_{12}$–$Ca_3Al_2Si_3O_{12}$ from their unit-cell measurements, in order to describe a small but important region of negative excess volume near the $Fe_3Al_2Si_3O_{12}$ end-member. Haselton and Newton (1980) fit a very similar negative excess volume region near $Mg_3Al_2Si_3O_{12}$ composition in the garnet join with $Ca_3Al_2Si_3O_{12}$ with a combined quadratic and gaussian curve. This empirical function has six parameters to be determined, and, in view of the relatively few molar volume measurements in this join, no statistical significance can be given to the derived parameters. However, the need to describe numerically the small but important anomaly encourages a break with previous tradition.

In this paper we further depart from tradition by considering the actual forms of molar volume–composition curves, rather than fitting simple equations to the data points. It will be shown that many binary silicate joins for which high-quality data are available have a significant region where excess volumes are smaller than in the mid-composition range and, indeed, are often negative. These excess volume "anomalies" fall into two general classes which allow structural interpretation based on individual crystal structures. The excess volume "anomalies" must be related to crystal structure "events" in the solid solution series, and these, in turn, may be related to small-scale peculiarities in the thermochemical properties of enthalpy, entropy, and free energy of formation.

Nepheline and the non-equivalent site (NS) substitution

Accurate unit-cell measurements of a series of solid solutions on the join $NaAlSiO_4$–$KAlSiO_4$ were presented by Smith and Tuttle (1957). Eleven compositions were carefully prepared by annealing glasses (made by J. F. Schairer) a few tens of degrees under the one-bar solidus. For compositions containing greater than 63% $KAlSiO_4$, there is a change to the kalsilite structure and a different molar volume trend. The measurements still stand as some of the best data available on binary silicate solutions.

Figure 1 shows the Smith and Tuttle (1957) data. Regardless of how one chooses to project the data to a fictive $KAlSiO_4$ nepheline end-member, it is clear that there is a broad region of negative excess volume (molar volume less than a proportional combination of the end-members) at the $NaAlSiO_4$ end. Smith and Tuttle chose to draw two straight lines to describe their data, intersecting at about 25 mole percent $KAlSiO_4$, but the data more properly describe a continuous curve with a somewhat sigmoidal aspect. Smith and Tuttle put forth a most plausible structural interpretation of the change of slope near the 25% $KAlSiO_4$ composition. The nepheline structure contains four sites per unit cell, capable of enclosing alkali metal ions. Of these four, one, the approximately 9-coordinated intraframework site, is significantly larger than the others, which are 8-coordinated. The larger site probably takes most of the K^+ in solid solution until it is saturated at about the 25% $KAlSiO_4$ composition. The response of the unit-cell volume is relatively small up to this point, since little expansion of the structure as a whole is required. When the large site is filled, the molar volume takes an immediate upswing, because the succeeding K^+ must enter smaller sites and must expand them to do so. In actual fact, the entropic drive toward partitioning of K^+ into the smaller sites in the dilute range causes progressive structural expansion, so that the K^+ saturation effect is not a cusp-like break but a smooth increase of slope.

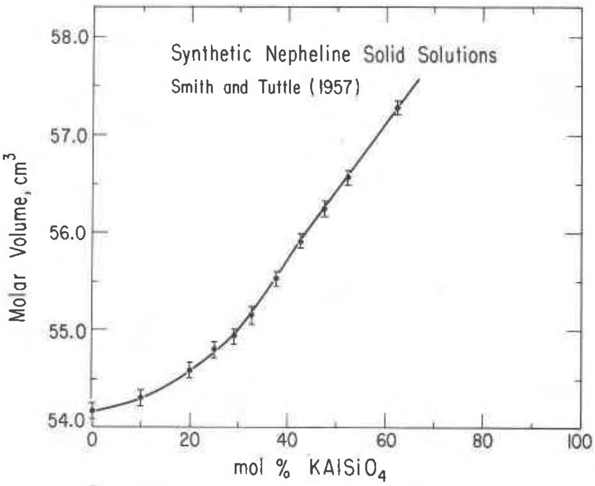

Fig. 1. Molar volumes of synthetic $(Na,K)AlSiO_4$ (nepheline) solid solutions (Smith and Tuttle, 1957), displaying non-equivalent site (NS) type of behavior. Brackets indicate error estimates.

The nepheline solid-solution series should not be considered an isolated instance. Many other solid-solution series occur in structures with similar but topologically non-equivalent cation sites of different sizes, and some of these sites will be better able to accept large-cation substituents than others. The result is a broadly sigmoidal molar volume curve with negative excess volume extending from the small-volume end-member to a rational mole fraction which expresses the fraction of the larger cation site among all sites capable of accepting a given substituent. There may well be a complementary but opposite region near the large-volume end-member where small mole fractions of a small substituent have only small effect on the molar volume. This kind of molar volume curve is expected to be of common occurrence and is here designated the non-equivalent-site (NS) type of substitution.

Garnet and the equivalent site (ES) substitution

Figure 2 shows the molar volume data for the almandine–grossular and pyrope–grossular joins. The striking feature is the small regions of negative excess volumes in both joins, giving rise to very asymmetric sigmoids. Attempts to fit the molar volume data by quadratic and cubic equations do not reproduce the sharply inflected regions, which are important because they lead to high partial molar volumes. These produce, in garnets of composition similar to many natural garnets, high activities of $Ca_3Al_2Si_3O_{12}$ component at elevated pressures.

The 24 divalent cation sites in the unit cell of garnet are topologically identical (Gibbs and Smith, 1966); therefore, initial reduced molar volume slopes do not have the same explanation as do nepheline solid solutions. A probable explanation was anticipated by Iiyama (1974). He attempted to model experimental studies of trace-element partitioning between micas, feldspars, and water vapor at elevated temperatures and pressures by assuming a random distribution of trace-element impurities in the synthetic micas and feldspars. He found, in fact, that the only reasonable interpretation of the partitioning data necessitated non-random mixing of the minor impurities in the host structure. As an explanation of the low entropy of mixing, Iiyama developed an "excluded volume" principle, in which an odd-sized trace-element ion deforms the local structure around it. This creates high free-energy gradients around the substituent and makes it less probable for another trace ion to enter the structure in its immediate neighborhood. For example, the data of distribution of Li^+ between coexisting muscovite and water vapor at 600°C and 1 kbar are best explained if a Li^+ ion does not enter the structure within a zone which includes about 15 alkali ions about another Li^+. Data for other trace ions in alkali feldspar and muscovite gave "excluded regions" of 10–350 alkali ions, depending on the structure and the impurity. The smallest excluded region was 3.3 alkali ions for Rb^+ substitution for Na^+ in nepheline, which is interesting in connection with the preceding discussion

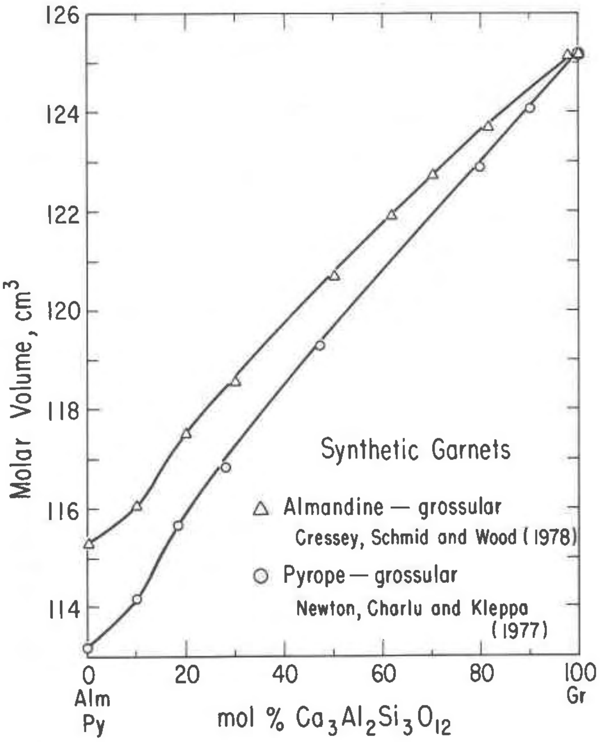

Fig. 2. Molar volumes of synthetic $Fe_3^{2+}Al_2Si_3O_{12}$–$Ca_3Al_2Si_3O_{12}$ garnets (Cressey *et al.*, 1978), and $Mg_3Al_2Si_3O_{12}$–$Ca_3Al_2Si_3O_{12}$ garnets (Newton *et al.*, 1977). Uncertainties in values somewhat smaller than sizes of symbols. Plot displays equivalent-site (ES) type of behavior.

about the enlarged cation site of one-quarter of the alkali ions. In a later paper, Iiyama and Volfinger (1976) modified the theory to allow that foreign ions can penetrate the "forbidden regions" after the structure becomes saturated with "forbidden regions," so that the structure as a whole begins to swell or shrink.

We postulate here that, when in a structure no ion site exists which is markedly larger than other similar ones which can accept a larger substituting ion, substitution into the structure behaves initially as an incompatible minor-element substitution, producing local deformations and "forbidden regions." Volume of mixing, as well as entropy of mixing, is less initially than at greater concentration. The structure as a whole does not undergo much expansion until the concentration of substituents reaches a point where they are close enough to interact substantially, at which point the structure must be capable of expansion, or else immiscibility will occur. We term this kind of substitution "equivalent site" (ES) substitution, and postulate that it will be of common occurrence in silicate binary joins which have only one site per unit cell for a substituting ion, or where two or more sites of substitution for the same ion are very similar in their properties, so that they behave as equivalent sites. For Ca substitution into Mg and Fe garnets, Figure 2 indicates that the foreign ions (Ca^{2+}) begin to interact significantly when their concentration is between 5 and 10 percent of the divalent cations. In the parlance of Iiyama (1974), the excluded region for this substitution comprises about 20 divalent cations. At concentrations less than this, Ca^{2+} ions tend not to share the same unit cell because of the high deformational free energy densities this would engender.

Unit-cell measurements of the pyrope–almandine, spessartine–almandine, and spessartine–grossular joins of sufficient detail to assess a volumetric ES-type substitution are not yet available. The spessartine–uvarovite (Naka *et al.,* 1975), uvarovite–andradite (Huckenholz and Knittel, 1976) and grossular–andradite (Huckenholz *et al.,* 1974) joins all show definite negative excess volumes near the smaller-volume end-members. Of all the detailed published volume data, only those for grossular–uvarovite (Huckenholz and Knittel, 1975) show no hint of a negative excess-volume effect, but are perfectly linear between end-members.

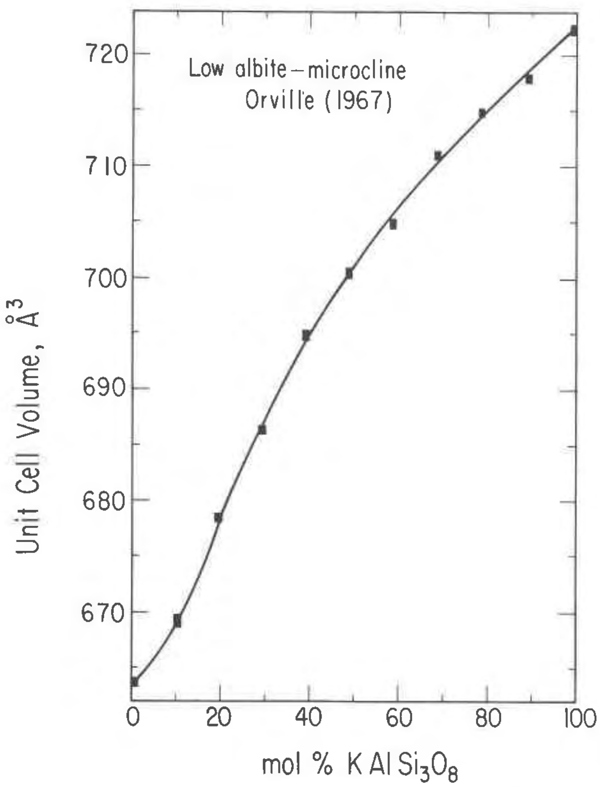

Fig. 3. Unit-cell volumes of exchanged $NaAlSi_3O_8$ (low albite)-$KAlSi_3O_8$ (microcline) solid solutions. Symbol sizes indicate Orville's (1967) uncertainty estimates.

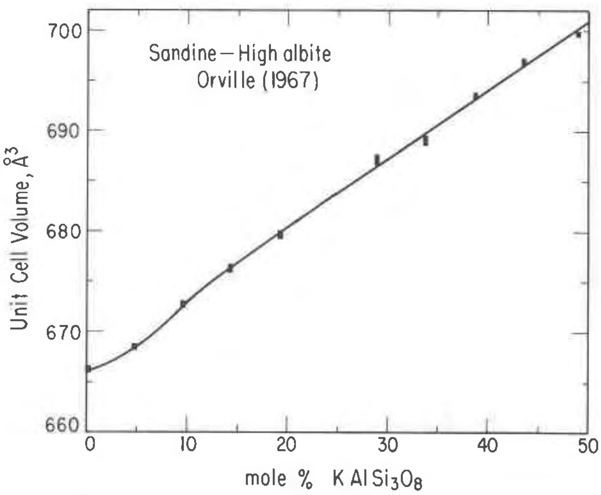

Fig. 4. Unit-cell volumes of synthetic high albite–sanidine solid solutions (Orville, 1967) to 50 mole percent $KAlSi_3O_8$. Sizes of symbols indicate author's uncertainty estimates.

Feldspars

Figure 3 shows the unit-cell volume data of Orville (1967) on low-albite microcline solid solutions which were prepared by alkali-exchanging a natural well-ordered $KAlSi_3O_8$ microcline. If the data points are connected faithfully rather than by a polynomial fit, there is a strong suggestion of an ES effect for K^+ substitution in low albite. Orville fitted his volume data with a quadratic function, which works very well for the majority of the points but completely misses the points at about one and ten percent.

Although there are two topologically distinct alkali sites in the unit cells of the triclinic alkali feldspars, these are extremely similar and would not be expected to show effects like preferential alkali ion site partitioning. We propose that K^+ ions on the roughly seven-coordinated low-albite alkali sites behave as incompatible ions (in terms of volume) until significant concentrations are reached, at which point a gradual coordination change to approximately 9-fold in microcline takes place with further substitution.

Figure 4 shows part of Orville's (1967) unit-cell volume measurements on a series of sanidine–high albite solid solutions crystallized from glasses at 800°C and one bar H_2O pressure for 5 to 7 days. There is again a suspicion of a negative excess volume very near the high albite end-member. It might be argued that a straight line can be fitted to all of the data to 50 mole percent which hits most of the measured points and from which the points at 29 and 34 mole percent have almost as great deviations as the point at 5 mole percent. However, the former two points have the greatest uncertainties of any of the cell volumes (0.35Å^3 compared to an average of 0.17), whereas the uncertainty in the volume of the 5 mole percent determination is 0.19Å^3. Also, comparison with the low albite–microcline curve of Figure 3, and recognition of negative excess entropy at very low K^+ concentration, to be discussed later, make it seem probable that a negative excess volume of the ES type does indeed occur in the high albite–sanidine series.

Unit-cell measurements on plagioclase synthesized from glass at 1200°C and 20 kbar (Newton *et al.*, 1980) are suggestive of an ES sigmoid volume relation; however, precision of the measured volumes is too low to exclude ideal mixing or other interpretations.

Olivine

Louisnathan and Smith (1968) carefully measured unit-cell volumes of a large number of natural accurately-analyzed olivines, shown in Figure 5. A negative excess volume of the ES type seems definitely to be present. Low concentrations of Mn^{2+} and Ca^{2+} in the high-Mg olivines are not large enough nor systematic enough to account for the deviation from the otherwise linear trend.

Recently, Schwab and Küstner (1977) have measured the unit-cell parameters of a series of synthetic samples on the Mg_2SiO_4–Fe_2SiO_4 join by high-precision Guinier powder photography. Their samples were made by annealing loose powders of mechanically-mixed oxides in air at 1160°–1400°C under an atmosphere with P_{O_2} on the iron–wüstite buffer. Iron was introduced as metallic iron and hematite. They mention that some of their samples were chemically analyzed but give no details. The unit-cell volumes are in good agreement with those of Louisnathan and Smith (1968) except that there seems to be no region of negative volume deviations. However, there are no data in the critical region of 6 to 13.5 percent Fe_2SiO_4. Within the uncertainties of the determinations, a region of concave-upward curvature is allowable, as with the natural olivines. The unit-cell data of Matsui and Syono (1968) on synthetic (Mg,Fe^{2+}) olivines are not sufficiently detailed to prove or disprove an ES effect. Thus, the presence or absence of a negative excess volume in olivine awaits final verification.

Matsui and Syono present unit-cell volume data for $(Ni,Mg)_2SiO_4$ olivines synthesized at high pressures and temperatures. Unlike the $(Fe,Mg)_2SiO_4$ olivines, the volume curve seems to be broadly sigmoidal, of the NS type. The $(Co,Mg)_2SiO_4$ series shows a similar but less marked excess volume. The differences between Fe–Mg, Co–Mg, and Ni–Mg olivines can readily be explained in terms of the site preferences of the three transition-metal ions. For Fe^{2+} and Mg, the two olivine sites are essentially equivalent and almost no cation ordering is observed (Rajamani *et al.*, 1975). Therefore, the only observable volume effect would be of the ES type. The other transition-metal ions, on the other hand, do have some preference for the smaller M1 position in olivine because of the higher crystal field stabilization energy (CFSE) that it confers on such ions (Wood, 1974). The order of magnitude of the CFSE effect should be $Ni^{2+} > Co^{2+} > Fe^{2+}$. Thus, one can predict that Ni^{2+} should have a pronounced preference for M1, Co^{2+} a less pronounced preference, and Fe^{2+} little or no preference. The expected Ni^{2+} octahedral site preference is demonstrated by X-ray dif-

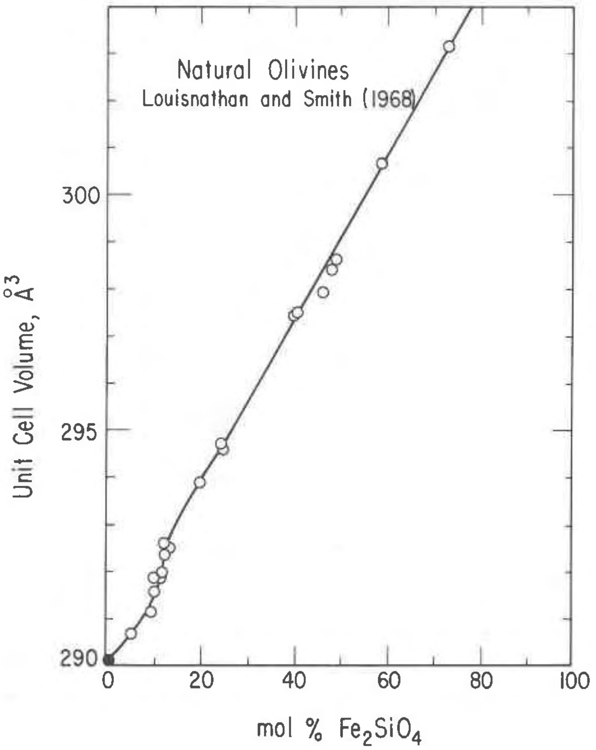

Fig. 5. Unit-cell volumes of natural analyzed Mg_2SiO_4–$Fe_2^{2+}SiO_4$ olivines (Louisnathan and Smith, 1968). Uncertainties in determinations somewhat smaller than sizes of symbols. Data set partially truncated for pictorial convenience. Filled circle is value for synthetic pure Mg_2SiO_4 given by Louisnathan and Smith.

fraction work (Rajamani *et al.*, 1975). $(Ni,Mg)_2SiO_4$ olivines would therefore be expected to exhibit a volume anomaly of the NS type, rather than of the ES type, exactly as observed.

The $(Ca,Mg)_2SiO_4$ olivines have limited solid solution ranges near the forsterite and monticellite ($CaMgSi_2O_4$) end members. The monticellite structure has Ca entirely ordered in the large M2 site, and this should be true of the solid solutions also. Therefore one should expect only an ES effect for one-site substitution. The volume data of Warner and Luth (1973) on the limited solid-solution ranges synthesized at 1450°C confirm this expectation.

Pyroxenes

Fe^{2+} substitution for Mg in synthetic orthopyroxenes produces a nearly linear unit-cell behavior, according to measurements on samples made from oxide mixes at high temperatures and pressures by Matsui *et al.* (1968) and Turnock *et al.* (1973). The Matsui *et al.* data are somewhat smoother and seem to show an ES effect (Fig. 6), while the Turnock *et al.* (1973) data do not. Both data sets strongly suggest a small change of slope at about 50 mole percent $FeSiO_3$, which is the behavior expected of a two-site NS series where one site has only a moderate preference for Fe^{2+}. The larger M2 octahedral site in orthopyroxene can accept Fe^{2+} more readily than can M1, as shown by the partitioning found in the Mössbauer spectroscopic studies of Virgo and Hafner (1969). The partitioning decreases somewhat with increasing temperature in the range 500°–1000°C, but, curiously, does not decrease above 1000°C, which means either that some crystal-chemical event occurs which impedes further M1 substitution or, more probably, that site-transfer kinetics are so fast above 1000°C that equilibrium partitioning cannot be quenched in by ordinary methods. Thus for samples prepared at 1000°C and above, there is still considerable segregation of Fe^{2+} into the M2 site at the lower Fe^{2+} concentrations. Orthopyroxene is one of the few systems which possibly shows both an ES and an NS effect.

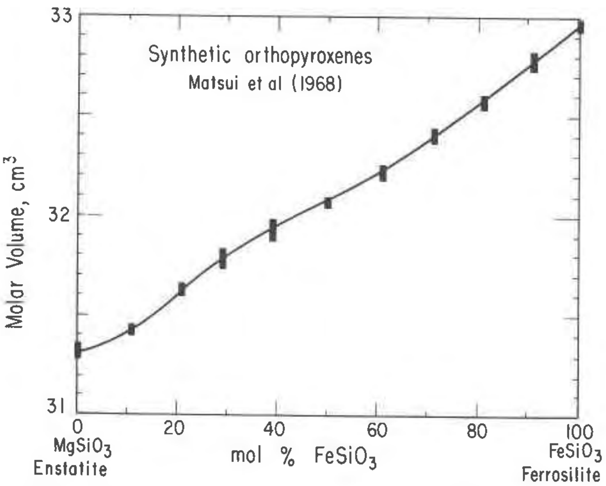

Fig. 6. Molar volumes of synthetic $(Mg,Fe^{2+})SiO_3$ orthopyroxenes (Matsui *et al.*, 1968). Symbol heights indicate uncertainty estimates.

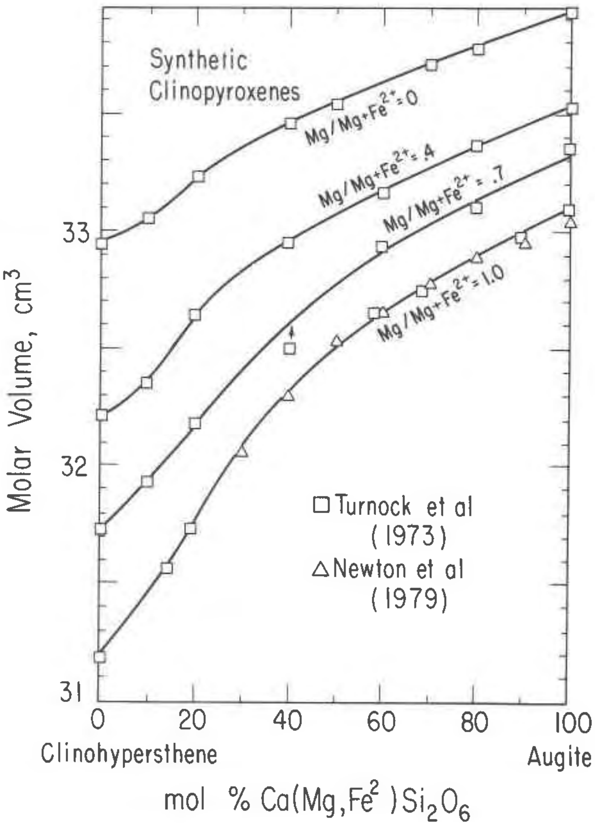

Fig. 7. Molar volumes of synthetic clinohypersthene–augite series, $(Mg,Fe^{2+})SiO_3$–$Ca_{0.5}(Mg,Fe^{2+})_{0.5}SiO_3$ (Turnock *et al.*, 1973), with some data of Newton *et al.* (1979) for the Fe-free system. Standard errors in determinations about the sizes of symbols.

Ca^{2+} substitution into (Mg,Fe^{2+}) clinopyroxenes produces more pronounced non-ideality. Figure 7 shows volume *vs.* composition in synthetic clinohypersthene–augite series of fixed Mg/Fe ratio, according to the measurements of Turnock *et al.* (1973) and some of Newton *et al.* (1979). The series appear to be of the ES type, with an increase of slope at less than 10 mole percent substitution of $Ca(Mg,Fe^{2+})Si_2O_6$. The curves are understandable if Ca^{2+} goes into only the M2 site. Small concentrations of Ca^{2+} produce localized deformations of the approximately 6-coordinated M2 clinohypersthene site, but higher concentrations force a structural expansion, with a conversion to the *C2/c* diopside structure, in which the M2 site has an approximate 8-fold coordination. Ohashi *et al.* (1975) found that the space group of synthetic $CaFe^{2+}Si_2O_6$–$Fe^{2+}Si_2O_6$ clinopyroxenes is completely converted from $P2_1/c$ to $C2/c$ at about 40 percent Ca substitution in M2.

Substitution on the $CaMgSi_2O_6$–$CaFe^{2+}Si_2O_6$ join produces an almost linear volume curve, according to the data of Turnock *et al.* (1973), although the points are somewhat scattered.

Substitution on the join $CaMgSi_2O_6$–$CaAl_2SiO_6$(CaTs) produces a slight negative deviation from volume linearity without fine-structure, according to the data on high-temperature, high-pressure synthetics of Clark *et al.* (1962) and Newton *et al.* (1977). It is not clear what to expect here, since we have the unusual substitution of a large ion (Al for Si in tetrahedral sites) and a small ion (Al for Mg in octahedral sites) simultaneously.

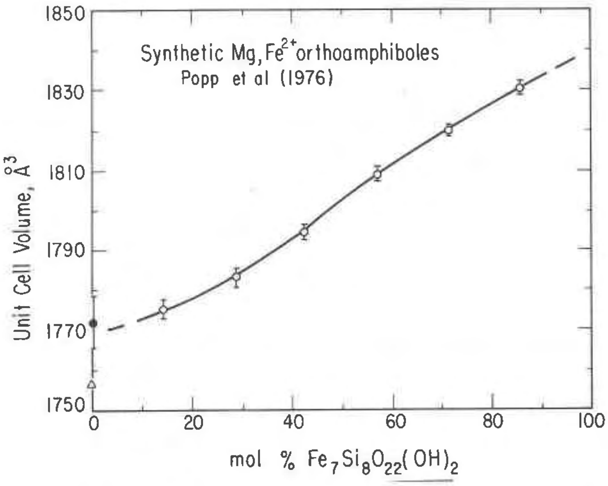

Fig. 8. Unit-cell volumes of synthetic (Mg,Fe^{2+}) orthoamphiboles (Popp *et al.*, 1976). Brackets show uncertainties of individual determinations. Triangle shows unit-cell volume of synthetic pure Mg-anthophyllite given by Greenwood (1963), and filled circle gives the recalculation of the anthophyllite unit-cell volume by Cameron (1975).

Amphiboles

Popp *et al.* (1976) made a careful study of unit-cell volumes in their synthetic $(Mg,Fe^{2+})_7Si_8O_{22}(OH)_2$ orthoamphibole series. The amphiboles were synthesized from oxides hydrothermally at 2 kbar and 650°–820°C with quartz–fayalite–magnetite and CH_4-graphite buffers. Recycling of charges was necessary to get nearly complete reaction, and measurements were made only on charges that were more than 95% amphibole. The data in Figure 8 show a relationship of the NS type, broadly sigmoidal with an increase of slope at about 30 mole percent of the iron end-member. Plotted also are data for synthetic Mg-anthophyllite (Greenwood, 1963). Cameron (1975) suspected that some of Greenwood's X-ray peaks were misindexed. He reindexed them and recomputed the molar volume from Greenwood's *d*-spacings, with the result shown in Figure 8, which enhances the sigmoidal aspect.

Figure 8 can be understood in terms of M-site partitioning of Mg and Fe^{2+}. Seifert (1978) showed, by Mössbauer spectroscopy of natural anthophyllites, that Fe^{2+} is partitioned very strongly into one of the four M sites, M4. This site will be effectively saturated at 28.6 mole percent of ferroanthophyllite. At greater iron concentrations, the other M sites, which are nearly identical in character (Seifert, 1978), must accept Fe^{2+}, with an overall structural expansion.

Critical data for the calcic and sodic amphibole series are lacking.

Micas

Hewitt and Wones (1975) prepared a large number of synthetic biotites in the quadrilateral aluminous eastonite $[KMg_2Al_3Si_2O_{10}(OH)_2]$–aluminous siderophyllite $[KFe^{2+}_2Al_3Si_2O_{10}(OH)_2]$–phlogopite $[KMg_3AlSi_3O_{10}(OH)_2]$–annite $[KFe^{2+}_3AlSi_3O_{10}(OH)_2]$. The syntheses were hydrothermal from oxides, generally under 100 bars H_2 pressure and one kbar total pressure.

Mg–Fe^{2+} substitution produces a nearly linear volume effect over a large range at fixed octahedral aluminum content. This is to be expected of an effectively one-site substitution with relatively small difference in unit-cell volume between the end-members. Data in the range 0–20 mole percent of Mg/(Mg + Fe^{2+}), which are necessary to check for an ES effect, were not presented.

Octahedral aluminum substitution at various fixed Mg/(Mg + Fe^{2+}) ratios is shown in Figure 9. The curves are NS-type sigmoids with increases in slope between 60 and 70% replacement of octahedral Al. Hewitt and Wones pointed out that the non-linearity might be associated with the fact that one-third of the octahedral cation sites in the biotite structure are significantly smaller than the others, and hence will favor Al occupancy, an interpretation quite in line with the present one.

Although a number of data exist on the unit-cell volumes of synthetic muscovite–paragonite $[KAl_3Si_3O_{10}(OH)_2$–$NaAl_3Si_3O_{10}(OH)_2]$ micas (Eugster

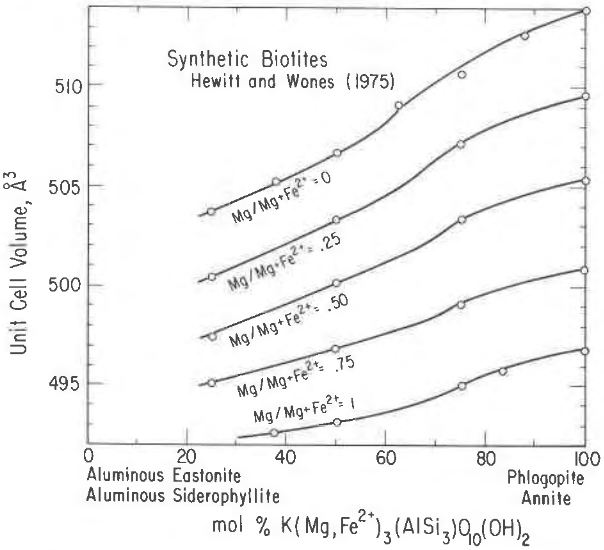

Fig. 9. Unit-cell volumes of synthetic biotites of various Mg/(Mg + Fe^{2+}) ratios on the join $K(Mg,Fe^{2+})_3AlSi_3O_{10}(OH)_2$ (phlogopite–annite)–$K(Mg,Fe^{2+})_2Al_3Si_2O_{10}(OH)_2$ (aluminous eastonite–aluminous siderophyllite). Uncertainties about those of symbol sizes. Some subjectivity of present authors exercised in drawing connecting lines. NS volume effect with change of slope at about 65 percent phlogopite–annite displayed (see text).

et al., 1972; Blencoe, 1977), the values at a given bulk composition show considerable dependence on the temperature and pressure of the synthesis and the predominant polytype present. For solid solutions synthesized under a specified set of conditions, the 1M micas synthesized at 8 kbar P_{H_2O} show a definite negative excess volume adjacent to the paragonite end-member, while 1M micas synthesized at lower pressures and the $2M_1$ micas do not. Chatterjee and Froese (1975) chose to represent the volume behavior of the $2M_1$ series with a curve interpolated between the carefully-measured volumes of the synthetic end-members (Chatterjee, 1974; Chatterjee and Johannes, 1974) with the cell volumes of a few analyzed well-characterized natural $2M_1$ micas. Their curve is substantially sigmoidal, with even larger negative excess volumes than the Blencoe (1977) 8 kbar 1M micas. Because of these apparent contradictions, the presence or absence of an ES volume effect in white mica cannot be decided yet.

Chlorite

An extensive experimental study of the synthetic join clinochlore, $Mg_5Al_2Si_3O_{18}(OH)_8$–daphnite, $Fe_5Al_2Si_3O_{18}(OH)_8$ was made by McOnie *et al.* (1975) at 2.07 kbar water pressure and 530° to 800°C. Their synthetic intermediate chlorites have unit-cell volumes which describe a straight line between the end-members, but with what appears to be a substantial negative excess volume adjacent to the clinochlore-end-member. It is difficult to be certain if the deviation is significant because some of the intermediate (Fe,Mg) chlorites show appreciable scatter about the linear trend. One possible interpretation of the scatter is that the chlorites may contain variable amounts of Fe^{3+}.

Cordierite

High-quality measurements for analyzed and characterized synthetic cordierite are not yet available. However, a few reliable data are available for well-characterized and chemically analyzed natural cordierite. Figure 10 shows the unit-cell volume behavior for some intermediate natural cordierites with negligible departures from the $(Mg,Fe^{2+})_2Al_4Si_5O_{18}\cdot nH_2O$ join. These are "perdistortional" (Miyashiro, 1957) with $\Delta = 0.21$–0.27. Variable channel H_2O has no effect on the unit-cell constants (Schreyer and Yoder, 1964).

The most unusual negative excess volume requires special explanation: a broad NS-type trend with the strong suggestion of a contraction of the unit cell with initial substitution of the large-volume component. This can possibly be understood if some Fe^{2+} resides in the structural channels. According to the

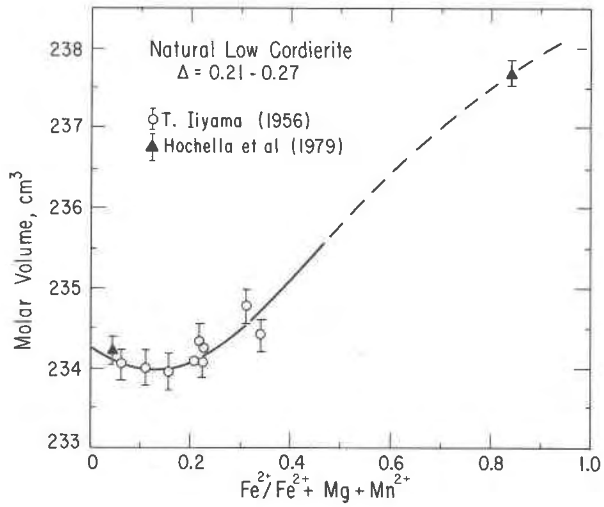

Fig. 10. Molar volumes of natural low (perdistortional) cordierites, $(Mg,Fe^{2+})_2Al_4Si_5O_{18}\cdot nH_2O$, from Iiyama (1956) and Hochella *et al.* (1979). The "distortion indices" (Miyashiro, 1957) are in the maximal range, $\Delta = 0.21$–0.27. Brackets indicate uncertainties in unit-cell volume determinations. The trend seems to show a contraction of the unit cell with the initial substitution of the large-volume end-member, which is a unique behavior for silicates.

Mössbauer resonance study of Duncan and Johnson (1974), as much as 40% of the iron may be in the continuous channel network. Goldman *et al.* (1977) interpreted their own Mössbauer spectra of several natural intermediate cordierites and verified the channel occupancy by Fe^{2+}, but estimated the amount at about one-tenth that found by Duncan and Johnston. The capacity for relatively highly-charged ions occupying the channelways is probably very limited. Thus iron substitution greater than a certain small percentage enters entirely into the normal octahedral sites, with expansion of the structure, as suggested by Figure 10.

Other silicate systems

The volume data of synthetic $Ca_2Al_2SiO_7$ (gehlenite)–$Ca_2MgSi_2O_7$ (akermanite) melilites show a small continuous negative excess volume across the join (Andrews, 1948; Neuvonen, 1952). According to the thermodynamic analysis of Waldbaum (1973), Mg is ordered into one tetrahedral site in all compositions, so that this site enlarges as $Ca_2MgSi_2O_7$ is approached. Simultaneously, there is a contraction associated with Si substitution for Al. The overall effect is a small negative excess volume. The kind of substitution and the volume behavior produced are somewhat similar to the join $CaAl_2SiO_6$–$CaMgSi_2O_6$, except that the Mg is octahedrally coordinated in the aluminous diopsides.

Seki (1959) gave accurate unit-cell data for four analyzed samples of epidote of variable Al/Fe^{3+} ratios, and two low-Fe^{3+} zoisites. Fe^{3+} substitution for Al appears to cause an almost perfectly linear unit-cell enlargement, a result which appears to be quite unusual for silicate substitutions.

Cr^{3+} substitution for Al in synthetic kyanite prepared at high pressures and temperatures (Langer and Seifert, 1971) produces a small curvature in the unit-cell volume curve adjacent to the Al_2SiO_5 end-member. The solid solutions of Fe^{3+} and V^{3+} in kyanite are not extensive enough to assess the unit-cell behavior (Langer and Frentrup, 1973).

Non-silicates

Are the ES and NS volume effects, which are displayed in the majority of binary silicate solid solutions, present also in other solid solutions? To explore this problem we have made a cursory survey of various non-silicate binary joins where there are extensive solid solutions and accurate volume measurements, preferably on composition-controlled synthetic samples.

The synthetic $(Fe^{2+}Mg)TiO_3$ ilmenites are one of the best documented synthetic systems available. Figure 11 shows the accurately-refined unit-cell volumes of 13 synthetic samples synthesized at high temperatures and pressures, with the compositions measured by electron microprobe (Bishop, 1976). An ES effect is present. The ilmenite structure is very much like that of corundum, but with layers of Ti-bearing octahedra alternating with Fe^{2+}-bearing octahedra along the [111] crystallographic direction in a perfectly ordered array (Lindsley, 1976). The Mg's substitute only for the Fe^{2+}'s, so that only an equivalent-site volume effect is anticipated.

The $FeTiO_3$–Fe_2O_3 (ilmenite–hematite) and Fe_2TiO_4–Fe_3O_4 (ulvöspinel–magnetite) joins have large negative excess-volume effects (Lindsley, 1965). The latter has a profoundly sigmoidal curve of the NS type. This can readily be understood by considering the nature of the sites in the crystals of the series. In $Fe_2^{2+}TiO_4$, Ti^{4+} ions occupy octahedral sites and Fe^{2+} ions are evenly divided between both oc-

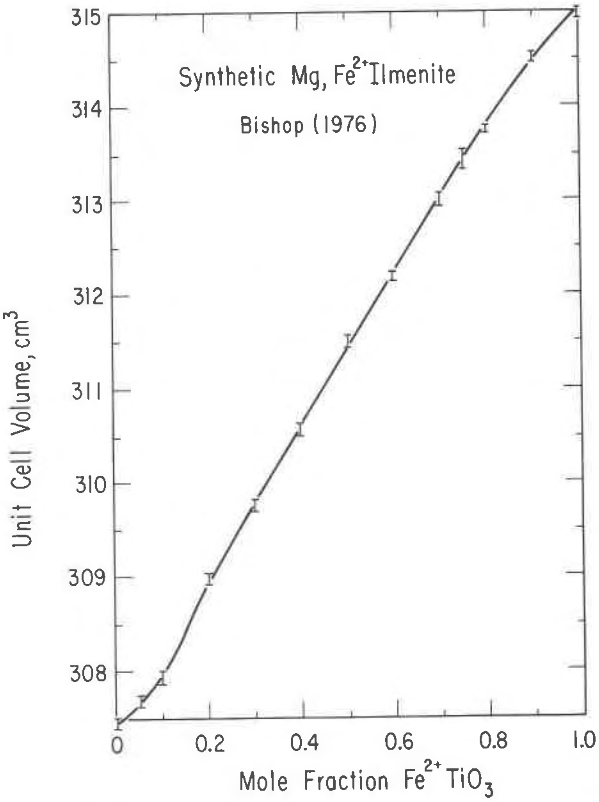

Fig. 11. Unit-cell volumes in the synthetic series $MgTiO_3$ (geikilite)–$Fe^{2+}TiO_3$ (ilmenite) (Bishop, 1976). Compositions were determined by microprobe analysis and brackets show error limits of unit-cell determinations. This is an example of a well-displayed ES volume effect in a non-silicate series.

tahedral and tetrahedral sites. In Fe_3O_4, Fe^{2+} ions occupy only octahedral sites, while Fe^{3+} ions occupy both tetrahedral and octahedral sites. Stephenson (1969) has shown that in the titanomagnetite solid solutions Fe^{3+} has a distinct preference for the tetrahedral sites. To a first approximation, then, both Fe^{2+} ions in the $Fe_2^{2+}TiO_4$ component tend to displace Fe^{3+} from octahedral coordination, leaving Fe^{3+} concentrated in the tetrahedra, until the octahedra are saturated with Fe^{2+}, with expansion of the structure as a whole. The result is a broad NS type of volume behavior.

The CaO–MgO and CaO–NiO systems show quite limited solid solutions excepts at very high temperatures. Both systems have initial substitutional volume behavior that suggests profoundly S-shaped volume curves (Doman *et al.*, 1963; Smith *et al.*, 1969). The samples were made at very high temperatures (2350°C for the CaO–MgO system) and there must be a high density of thermal defects, so that the principles derived from the silicate volume relations have somewhat dubious application.

The Al_2O_3–Cr_2O_3, Cr_2O_3–Fe_2O_3, and Al_2O_3–Fe_2O_3 joins are completely miscible at one bar and high temperatures. A very complete and accurate study of the volume relations (Steinwehr, 1967) shows only small, symmetrically positive deviations from linearity for all three joins. The $MgAl_2O_4$–Al_2O_3 (spinel–γ-alumina) join shows continuous negative departures from linearity (Viertel and Seifert, 1979).

$CaCO_3$–$MgCO_3$ rhombohedral carbonates show the expected positive excess volumes near the $CaCO_3$ end (Goldsmith and Graf, 1958). Critical data for the Mg-rich portion, which has very limited solid solution with $CaCO_3$, are lacking. The $BaCO_3$–$CaCO_3$ aragonite-structure series and the $SrCO_3$–$CaCO_3$ calcites seem to show perfect volume linearity, and the $BaCO_3$–$SrCO_3$ and $BaCO_3$–$CaCO_3$ rhombohedral carbonates show continuously negative departures (Chang, 1965). Brice and Chang (1973) present only the d_{104} spacings of some syntheses on the $MgCa(CO_3)_2$–$MgSr(CO_3)_2$ and $MgSr(CO_3)_2$–$MgBa(CO_3)_2$ dolomite joins. Both data sets are suspiciously sigmoidal, though the authors drew straight lines through the data.

FeS substitution in synthetic ZnS (sphalerite) shows only slight positive deviation from linearity throughout the extensive solid-solution region (Barton and Toulmin, 1966).

The available evidence indicates that the volume behavior of non-silicate species is not as characteristically sigmoidal as in silicates. It can, however, occur in certain structures, with predictive principles yet to be determined.

Related thermodynamic consequences and "anomalies"

A direct consequence of the sometimes sharp curvature of the volume–composition curves of many silicate solutions is the effect on the activities of the components at elevated pressures, according to the relation:

$$\left(\frac{\delta \ln \alpha_i}{\delta P}\right)T = \frac{\overline{V}_i - V_i}{RT}$$

where α_i is the activity of the ith component, $\overline{V_i}$ is its partial molal volume, V_i its molar volume, and P, T, and R are, respectively, the pressure, temperature, and gas constant. The ES effect substantially increases the activity of $Ca_3Al_2Si_3O_{12}$ in garnet in the range 10–20 mole percent, which is the concentration range of many garnets from deep-seated granulites and peridotites.

As an example of the operation of the partial molal volume effect on the activity of $Ca_3Al_2Si_3O_{12}$, Table 1 gives the one-bar activity coefficients (ratios of activities to concentrations) derived by Hensen *et al.* (1975) from phase equilibrium measurements at high temperatures and pressures in the system CaO–MgO–Al_2O_3–SiO_2. Because of restrictions from the reactions involved in the activity measurements, all

Table 1. Activity coefficients of $Ca_3Al_2Si_3O_{12}$ in pyrope-grossular garnet solutions, calculated from high-temperature, high-pressure phase equilibrium measurements (Hensen *et al.*, 1975) and from calorimetry (Haselton and Newton, 1980). The second γ column gives the Hensen *et al.* (1975) results corrected to one bar by the Cressey *et al.* (1978) partial molal volumes.

HSW (1975) run conditions T(K)	P(Kb)	X_{gr}	γ uncorr. 1 bar HSW	γ corr. 1 bar HSW,CSW	γ calor. 1 bar HN
1273	17.0	0.22	1.437	1.220	1.211
1273	17.0	0.20	1.656	1.217	1.262
1373	18.5	0.21	1.418	1.158	1.176
1373	17.3	0.16	1.527	1.271	1.299
1373	15.0	0.11	1.554	1.450	1.466
1473	19.0	0.19	1.287	1.096	1.164
1473	18.5	0.18	1.260	1.082	1.185
1473	16.5	0.12	1.406	1.336	1.340
1473	15.0	0.10	1.353	1.376	1.371
1573	21.0	0.22	1.153	1.038	1.070
1573	16.0	0.11	1.154	1.198	1.294

their synthetic garnets were in the range 10–22% $Ca_3Al_2Si_3O_{12}$. Solution calorimetry and adiabatic heat capacity measurement of synthetic pyrope–grossular solutions also make possible calculation of the one-bar activity coefficients (Haselton and Newton, 1980). Table 1 shows that the activity coefficients derived from the phase equilibrium measurements of Hensen *et al.* (1975) are in good agreement with the calorimetric ones, if they are corrected for the sharp ES-effect partial molal volume change of $Ca_3Al_2Si_3O_{12}$. They are, however, in much less good agreement if one assumes pressure independence of activities. The general principle illustrated in this example will apply to many other mineral systems and should be taken into account when extrapolating thermodynamic data in pressure–composition space.

The minor-element substitution theory of Iiyama (1974) and Iiyama and Volfinger (1976) postulates limited mixing of the "foreign" ions in the dilute range. One would thus expect a negative excess entropy adjacent to the small-ion end-member. Such an effect has been calculated for the sanidine–high albite series by Thompson and Hovis (1979) from a combination of enthalpy of solution and phase-equilibrium measurements. This is the only silicate system where both calorimetric and phase equilibrium data are sufficient to justify a search for such an effect. Our speculations on the ES-type substitution lead us to predict that this behavior should be quite common. In order to observe the effect, coverage in both types of measurements must be especially extensive in the region 0–10 mole percent of the large-volume component.

If an avoidance or excluded volume principle is operative, an ordering of out-sized ions may result, which, as W. L. Brown suggested in the discussion to Iiyama's (1974) paper, would give rise to superstructures identifiable by X-ray diffraction. Preliminary X-ray work on a single crystal of synthetic grossular$_{10}$pyrope$_{90}$ garnet (M. J. Dempsey, personal communication) indicates that there are some weak additional reflections which imply symmetry lower than *Ia*3*d*. This would be consistent with the presence of a superstructure in the garnet. It seems plausible that, when the fraction of the large substituting cations is near to a small "magic number," say 1/8 or 1/12, of the equivalent sites accepting the ion, the most effective method of mutual avoidance and minimizing of the structural deformation energy would be to order the large ions in particular sites, which can now be thought of as non-equivalent. This would produce a different (usually lower-symmetry) space group for a narrow range of compositions. Such a very local ordering event should in general be attended by an enthalpy anomaly, which must be exothermic enough to counteract the decrease of entropy in ordering. A smaller-than-average or even negative excess free energy of mixing should be the result. A free-energy anomaly of this type was found for grossular–almandine mixing in the low-Ca range by Cressey *et al.* (1978), based on their high-pressure, high-temperature phase equilibrium measurements. The enthalpy of solution measurements of Newton *et al.* (1977) were not spaced closely enough in the appropriate composition range to determine whether a similar anomaly occurs in the pyrope–grossular series.

A narrow-composition ordered region in a binary system may be fringed by two-phase regions in which an ordered and a disordered pair of solid solutions coexist (see for example the proposed diagram for the ordering of $CaMgSi_2O_6$–$NaAlSi_2O_6$ omphacites in Champness, 1973). The kind of ordering event we envision in the ES type of substitution may well produce very localized phase immiscibility in many systems. Evidence of this possibility has been found by electron-diffraction analysis of a natural Ca-bearing garnet. Cressey (1978) found apparent precipitates of grossular mole fraction 0.2 in a host garnet of grossular mole fraction 0.36 from a high-grade granulite. Although no difference in symmetry of the two phases could be found, the discrete two-garnet association suggests different structures.

The NS type of substitution may also be thought of as leading to compound formation in a certain sense, for, at the fractional "magic number" concentration where the easily-filled ion-site is saturated, the structure has a considerable degree of order. However, the enthalpy and free energy effects, if any, are not likely to be symmetrically disposed about the magic fraction, because a rapid increase in structural strain energy is anticipated on the high-concentration side of saturation. It is more likely that a broad region of relatively low excess free energy of mixing exists on the small-volume side of the rational fraction, reflecting the fact that it is easier to put a small ion in a large site than a large ion in a small site. This could be the reason for the small negative excess free energy of mixing region which Zyrianov *et al.* (1978) obtained for Na-rich nepheline solid solutions from experimental composition tie-lines with coexisting alkali feldspars. The anomaly is centered at a K^+ content somewhat lower than the "magic number" of 25 percent.

Acknowledgments

The research of R. C. Newton is supported by NSF grant EAR 78-15939, and that of B. J. Wood at the University of Chicago by the Materials Research Laboratory (NSF) program.

References

Andrews, K. W. (1948) The lattice parameters and interplanar spacings of some artifically prepared melilites. *Mineral. Mag., 28,* 374–379.

Barton, P. B. and P. Toulmin (1966) Phase relations involving sphalerite in the Fe–Zn–S system. *Econ. Geol., 61,* 815–849.

Bishop, F. C. (1976) *Partitioning of Fe^{2+} and Mg between ilmenite and some ferromagnesian silicates.* Ph.D. Thesis, Department of the Geophysical Sciences, University of Chicago, Chicago, Illinois.

Blencoe, J. G. (1977) Molal volumes of synthetic paragonite–muscovite micas. *Am. Mineral., 62,* 1200–1215.

Brice, W. R. and L. Y. Chang (1973) Subsolidus phase relations in aragonite-type carbonates. III. The system $MgCO_3$–$CaCO_3$–$BaCO_3$, $MgCO_3$–$CaCO_3$–$SrCO_3$, and $MgCO_3$–$SrCO_3$–$BaCO_3$. *Am. Mineral., 58,* 979–985.

Cameron, K. L. (1975) An experimental study of actinolite–cummingtonite phase relations with notes on the synthesis of Fe-rich anthophyllite. *Am. Mineral., 60,* 375–390.

Champness, P. E. (1973) Speculation on an order–disorder transformation in omphacite. *Am. Mineral., 58,* 540–542.

Chang, L. Y. (1965) Subsolidus phase relations in the system $BaCO_3$–$SrCO_3$, $SrCO_3$–$CaCO_3$, and $BaCO_3$–$CaCO_3$. *J. Geol., 73,* 346–368.

Chatterjee, N. D. (1974) X-ray powder pattern and molar volume of synthetic 2M-paragonite: a refinement. *Contrib. Mineral. Petrol., 43,* 25–28.

——— and E. Froese (1975) A thermodynamic study of the pseudobinary join muscovite–paragonite in the system $KAlSi_3O_8$–$NaAlSi_3O_8$–Al_2O_3–SiO_2–H_2O. *Am. Mineral., 60,* 985–993.

——— and W. Johannes (1974) Thermal stability and standard thermodynamic properties of synthetic $2M_1$-muscovite, $KAl_2[AlSi_3O_{10}(OH)_2]$. *Contrib. Mineral. Petrol., 48,* 89–114.

Clark, S. P., F. J. Schairer and J. de Neufville (1962) Phase relations in the system $CaMgSi_2O_6$–$CaAl_2SiO_6$–SiO_2 at low and high pressures. *Carnegie Inst. Wash. Year Book, 61,* 59–68.

Cressey, G. (1978) Exsolution in almandine–pyrope–grossular garnet. *Nature, 271,* 533–534.

———, R. Schmid and B. J. Wood (1978) Thermodynamic properties of almandine–grossular garnet solid solutions. *Contrib. Mineral. Petrol., 67,* 397–404.

Doman, R. C., J. B. Barr, R. N. McNally and A. M. Alper (1963) Phase equilibria in the system CaO–MgO. *J. Am. Ceram. Soc., 46,* 313–316.

Duncan, J. F. and J. H. Johnston (1974) Single-crystal ^{57}Fe Mössbauer studies of the site positions in cordierite. *Austr. J. Chem., 27,* 249–258.

Eugster, H. P., A. L. Albee, A. E. Bence, J. B. Thompson and D. R. Waldbaum (1972) The two-phase region and excess mixing properties of paragonite–muscovite crystalline solutions. *J. Petrol., 13,* 147–179.

Gibbs, G. V. and J. V. Smith (1966) Refinement of the crystal structure of pyrope. *Am. Mineral., 50,* 2023–2039.

Goldman, D. S., G. R. Rossman and W. A. Dollase (1977) Channel constituents in cordierite. *Am. Mineral., 62,* 1144–1157.

Goldsmith, J. R. and D. L. Graf (1958) Relation between lattice constants and composition of the Ca–Mg carbonates. *Am. Mineral., 43,* 84–101.

Greenwood, H. J. (1963) The synthesis and stability of anthophyllite. *J. Petrol., 4,* 317–351.

Haselton, H. T. and R. C. Newton (1980) Thermodynamics of pyrope–grossular garnets and their stabilities at high temperatures and pressures. *J. Geophys. Res., Kennedy Vol.,* in press.

Hensen, B. J., R. Schmid and B. J. Wood (1975) Activity–composition relations for pyrope–grossular garnet. *Contrib. Mineral. Petrol., 51,* 161–166.

Hess, H. H. (1952) Orthopyroxenes of the Bushveld type, ion substitutions and changes in unit cell dimensions. *Am. J. Sci., Bowen Vol.,* 173–187.

Hewitt, D. A. and D. R. Wones (1975) Physical properties of some synthetic Fe–Mg–Al trioctahedral biotites. *Am. Mineral., 60,* 854–862.

Hochella, M. F., G. E. Brown, F. K. Ross and G. V. Gibbs (1979) High-temperature crystal chemistry of hydrous Mg- and Fe-cordierites. *Am. Mineral., 64,* 337–351.

Huckenholz, H. G. and D. Knittel (1975) Uvarovite: stability of uvarovite–grossularite solid solution at low pressure. *Contrib. Mineral. Petrol., 49,* 211–232.

——— and ——— (1976) Uvarovite: stability of uvarovite–andradite solid solutions at low pressures. *Contrib. Mineral. Petrol., 56,* 61–76.

———, W. Lindhuber and J. Springer (1974) The join $CaSiO_3$–Al_2O_3–Fe_2O_3 of the CaO–Al_2O_3–FeO_3–SiO_2 quaternary system and its bearing on the formation of granditic garnets and fassaitic pyroxenes. *Neues Jahrb. Mineral. Abh., 121,* 160–207.

Iiyama, T. (1956) Optical properties and unit cell dimensions of cordierite and indialite. *Mineral. J., 1,* 382–394.

Iiyama, J. T. (1974) Substitution, déformation locale de la maille et équilibre de distribution des éléments en traces entre silicates et solution hydrothermale. *Bull. Soc. fr. Mineral. Cristallogr., 97,* 143–151.

——— and M. Volfinger (1976) A model for trace-element distribution in silicate structures. *Mineral Mag. 40,* 555–564.

Kerrick, D. M. and L. S. Darken (1975) Statistical thermodynamic models for ideal oxide and silicate solid solutions, with application to plagioclase. *Geochim. Cosmochim. Acta, 39,* 1431–1442.

Langer, K. and K. R. Frentrup (1973) Synthesis and some properties of iron- and vanadium-bearing kyanites, $(Al,Fe^{3+})_2SiO_5$. *Contrib. Mineral. Petrol., 41,* 31–46.

——— and F. Seifert (1971) High-pressure, high-temperature synthesis and properties of chromium kyanite, $(Al,Cr)_2SiO_5$. *Z. anorg. allg. Chem., 383,* 29–39.

Lindsley, D. H. (1965) Iron–titanium oxides. *Carnegie Inst. Wash. Year Book, 64,* 144–148.

——— (1976) The crystal chemistry and structure of oxide minerals as exemplified by the Fe–Ti oxides. In D. Rumble III, Ed., *Oxide Minerals.* Mineral Soc. Am. Short Course Notes, Vol. III, L1–L60.

Louisnathan, S. J. and J. V. Smith (1968) Cell dimensions of olivine. *Mineral. Mag., 37,* 1123–1134.

Matsui, Y. and Y. Syono (1968) Unit cell dimensions of some synthetic olivine group solid solutions. *Geochem. J., 2,* 51–59.

———, S. Akimoto and K. Kitayama (1968) Unit cell dimensions of some synthetic orthopyroxene group solid solutions. *Geochem. J., 2,* 61–70.

McOnie, A. W., J. J. Fawcett and R. S. James (1975) The stability of intermediate chlorites of the clinochlore–daphnite series at 2 kbar P_{H_2O}. *Am. Mineral., 60,* 1047–1062.

Miyashiro, A. (1957) Cordierite–indialite relations. *Am. J. Sci., 255,* 43–62.

Naka, S., Y. Suwa and T. Kameyama (1975) Solid solubility between uvarovite and spessartite. *Am. Mineral., 60,* 418–422.

Neuvonen, K. J. (1952) Thermochemical investigation of the akermanite–gehlenite series. *Bull. Geol. Comm. Finlande, 26,* 158, 5–50.

Newton, R. C., T. V. Charlu and O. J. Kleppa (1977) Thermochemistry of high pressure garnets and clinopyroxenes in the system $CaO–MgO–Al_2O_3–SiO_2$. *Geochim. Cosmochim. Acta, 41,* 369–377.

———, ——— and ——— (1980) Thermochemistry of the high structural state plagioclases. *Geochim. Cosmochim. Acta,* in press.

———, ———, P. A. M. Anderson and O. J. Kleppa (1979) Thermochemistry of synthetic clinopyroxenes on the join $CaMgSi_2O_6–Mg_2Si_2O_6$. *Geochim. Cosmochim. Acta, 43,* 55–60.

Ohashi, Y., C. W. Burnham and L. W. Finger (1975) The effect of Ca–Fe substitution on the clinopyroxene crystal structure. *Am. Mineral., 60,* 423–434.

Orville, P. M. (1967) Unit-cell parameters of the microcline–low albite and the sanidine–high albite solid solution series. *Am. Mineral., 52,* 55–86.

Popp, R. K., M. C. Gilbert and J. R. Craig (1976) Synthesis and X-ray properties of Fe–Mg orthoamphiboles. *Am. Mineral., 61,* 1267–1279.

Rajamani, V., G. E. Brown and C. T. Prewitt (1975) Cation ordering in Ni–Mg olivine. *Am. Mineral., 60,* 292–299.

Schreyer, W. and H. S. Yoder (1964) The system Mg-cordierite–H_2O and related rocks. *Neues Jahrb. Mineral. Abh., 101,* 271–342.

Schwab, R. G. and D. Küstner (1977) Präzisions-gitterkonstantenbestimmung zur Festlegung röntgenographischer Bestimmungskurven für synthetische Olivine der Mischkristallreihe Forsterit–Fayalit. *Neues Jahrb. Mineral. Monatsh.,* 205–215.

Seifert, F. (1978) Equilibrium Mg–Fe^{2+} cation distribution in anthophyllite. *Am. J. Sci., 278,* 1323–1333.

Seki, Y. (1959) Relation between chemical composition and lattice constants of epidote. *Am. Mineral., 44,* 720–730.

Smith, D. E., T. Y. Tien and L. H. Van Vlack (1969) The system NiO–CaO. *J. Am. Ceram. Soc., 52,* 459–460.

Smith, J. V. and O. F. Tuttle (1957) The nepheline–kalsilite system: I. X-ray data for the crystalline phases. *Am. J. Sci., 255,* 282–305.

Steinwehr, H. E. (1967) Gitterkonstanten im System α-(Al, Fe,Cr$)_2O_3$ und ihr Abweichen von der Vegardregel. *Z. Kristallogr., 125,* 377–403.

Stephenson, A. (1969) The temperature dependent cation distribution in titanomagnetites. *Geophys. J. Roy. Astr. Soc., 18,* 199–210.

Thompson, J. B. (1967) Thermodynamic properties of simple solutions. In P. H. Abelson, Ed., *Researches in Geochemistry,* Vol. II, p. 348–361. Wiley, New York.

——— and G. S. Hovis (1979) Entropy of mixing in sanidine. *Am. Mineral., 64,* 57–65.

Turnock, A. C., D. H. Lindsley and J. E. Grover (1973) Synthesis and unit cell parameters of Ca–Mg–Fe pyroxenes. *Am. Mineral., 58,* 50–59.

Viertel, H. U. and F. Seifert (1979) Physical properties of defect spinels in the system $MgAl_2O_4–Al_2O_3$. *Neues Jahrb. Mineral. Abh., 134,* 167–182.

Virgo, D. and S. Hafner (1969) Fe^{2+},Mg order–disorder in heated orthopyroxenes. *Mineral. Soc. Am. Spec. Pap., 2,* 67–81.

Waldbaum, D. R. (1973) The configurational entropies of $Ca_2MgSi_2O_7–Ca_2Al_2SiO_7$ melilites and related minerals. *Contrib. Mineral. Petrol., 39,* 33–54.

Warner, R. D. and W. C. Luth (1973) Two-phase data for the join monticellite ($CaMgSiO_4$)–forsterite (Mg_2SiO_4): experimental results and numerical analysis. *Am. Mineral., 58,* 998–1008.

Wood, B. J. (1974) Crystal field spectrum of Ni^{2+} in olivine. *Am. Mineral., 59,* 244–248.

Zyrianov, V. N., L. L. Perchuk and K. K. Podlesskii (1978) Nepheline–alkali feldspar equilibria: I. Experimental data and thermodynamic calculations. *J. Petrol., 19,* 1–44.

Manuscript received, October 11, 1979;
accepted for publication, December 5, 1979.